Effect of Particle Diameter on Silver Nanoparticle Aggregation and Dissolution in Aquatic Systems

Thesis

Presented in Partial Fulfillment of the Requirements for the Honors Research Distinction

By

Audrey Marie Stallworth

Undergraduate Program in Civil, Environmental, and Geodetic Engineering

The Ohio State University

2017

Thesis Committee:

Dr. John Lenhart, Advisor

Dr. Linda Weavers

Abstract

Silver nanoparticles (AgNPs) are used in many consumer products as an antibacterial agent. The small size of these particles means they are more reactive, because their surface area is larger. However, the widespread usage of AgNPs has consequently led to their release into the aquatic environment, where they have the potential to harm organisms that are not their intended target. Studies have been conducted on the fate and toxicity of AgNPs, but each study uses different sizes, calling into question the consistency of results across different sizes of AgNPs. In addition, a variety of sizes may be utilized in consumer products. One method of determining the behavior of AgNPs in the environment uses the addition of electrolytes to determine their effect on the dissolution and/or aggregation of AgNPs. This research focused on the effect of different concentrations of three different electrolytes ($NaNO_3$, $CaCl_2$ and NaCl) on the aggregation kinetics of three different sizes of citrate-coated silver nanoparticles (20 nm, 50 nm, 80 nm). It was hypothesized that AgNPs with a smaller initial particle size would be less stable than AgNPs with a larger initial particle size in the presence of electrolytes. After the addition of an electrolyte to a silver nanoparticle suspension, the change in size of the particles was measured over time (4 – 15 minutes) using Dynamic Light Scattering. Silver nanoparticles of all three sizes were found to be equally stable in $NaNO_3$ and

NaCl, and larger particles were more stable in $CaCl_2$. These results suggest that further investigation into the effect of AgNP size on aggregation may be necessary.

Acknowledgements

I would like to thank Dr. Lenhart for his support and guidance as an advisor, as well as the College of Engineering for allowing me the opportunity to pursue this research project.

Vita

June 2012……Newark Catholic High School

August 2012 to present……..Undergraduate Environmental Engineering student, The Ohio State University

Publications

Wei Zhou, Yen-Ling Liu, Audrey M. Stallworth, Chunsong Ye, and John J. Lenhart. Effects of pH, Electrolyte, Humic Acid, and Light Exposure on the Long-Term Fate of Silver Nanoparticles *Environ. Sci. & Technol*. 2016, (Web), DOI: 10.1021/acs.est.6b03237

Fields of Study

Major Field: Environmental Engineering

Minor Field: Environment, Economy, Development and Sustainability

Table of Contents

Abstract ii
Acknowledgements iv
Vita v
List of Tables viii
List of Figures ix
1. Introduction 1
2. Methods 6
2.1 Materials 6
2.2 Experiment 7
2.3 Aggregation Kinetics 8
3. Results 9
3.1 Characterization of Silver Nanoparticles 9
3.2 Aggregation and Dissolution of Silver Nanoparticles in Sodium Nitrate 12
3.2.1 Aggregation and Dissolution of 20 nm Silver Nanoparticles in Sodium Nitrate 12
3.2.2 Aggregation and Dissolution of 50 nm Silver Nanoparticles in Sodium Nitrate 15
3.2.3 Aggregation and Dissolution of 80 nm Silver Nanoparticles in Sodium Nitrate 16
3.3 Aggregation and Dissolution of Silver Nanoparticles in Sodium Chloride 17
3.3.1 Aggregation and Dissolution of 20 nm Silver Nanoparticles in Sodium Chloride 17
3.3.2 Aggregation and Dissolution of 50 nm Silver Nanoparticles in Sodium Chloride 19
3.3.3 Aggregation and Dissolution of 80 nm Silver Nanoparticles in Sodium Chloride 20
3.4 Aggregation and Dissolution of Silver Nanoparticles in Calcium Chloride 20
3.4.1 Aggregation and Dissolution of 20 nm Silver Nanoparticles in Calcium Chloride 20
3.4.2 Aggregation and Dissolution of 50 nm Silver Nanoparticles in Calcium Chloride 23

3.4.3 Aggregation and Dissolution of 80 nm Silver Nanoparticles in Calcium Chloride 23
4. Discussion 24
4.1 Critical Coagulation Concentration Trends for $NaNO_3$ and NaCl 24
4.2 Critical Coagulation Concentration Trend for $CaCl_2$ 27
5. Conclusion 28
6. References 30
Supporting Information 34
Raw Data: DLS Readings for 20, 50 and 80 nm AgNPs, k_{exp} values, k_{fast} values 34
Size versus time plots and 1/W (“alpha”) versus electrolyte concentration for each AgNP size and electrolyte combination 37

List of Tables

Table 1: Characteristics of AgNPs 10
Table 2: CCC Values for 20, 50 and 80 nm AgNPs 24
Table 6: Stock AgNP DLS measurements 34
Table 7: Aggregation kinetics data for 80 nm AgNPs 34
Table 8: Aggregation kinetics data for 50 nm AgNPs 35
Table 9: Aggregation kinetics data for 20 nm AgNPs 36

List of Figures

Figure 1: UV-vis peaks for stock 20, 50 and 80 nm AgNPs after dialysis 11
Figure 2: Stability of 20, 50 and 80 nm AgNPs in $NaNO_3$ 13
Figure 3: Initial Dissolution of 20, 50 and 80 nm AgNPs in $NaNO_3$ 14
Figure 4: 20 nm AgNPs after the addition of NaNO3 14
Figure 5: Stability of 20, 50 and 80 nm AgNPs in NaCl 18
Figure 6: Initial Dissolution of 20, 50 and 80 nm AgNPs in NaCl 18
Figure 7: Stability of 20, 50 and 80 nm AgNPs in $CaCl_2$ 21
Figure 8: Initial Dissolution of 20, 50 and 80 nm AgNPs in $CaCl_2$ 22

1. Introduction

Silver has been used as an antibacterial agent for centuries. It was most commonly used as an antiseptic agent in the form of silver nitrate to prevent eye infections and in the form of silver sulphadiazine to prevent the infection of burn wounds in the 1900s (Maillard and Hartemann 2013). Silver antibacterial agents get their bactericidal properties from their release of silver ions, or Ag^+. Silver ions are antibacterial via multiple pathways; they can interfere with the cell membrane and respiration, and they can disrupt cell metabolism, usually resulting in cell death (Maillard and Hartemann 2013). In recent years, the use of silver nanoparticles (AgNPs), or silver particles with diameters smaller than 100 nm, has emerged and increased. These AgNPs can still be found in traditional uses such as on wound dressings and on implants as an antiseptic, and additionally in consumer products such as socks or toothpaste as an antibacterial agent, or in industrial applications such as water treatment membranes in order to avoid biofouling (Maillard and Hartemann 2013, Zodrow et al 2009). Silver nanoparticles are preferred because their small size maximizes their surface area to volume ratio, increasing their reactivity and efficacy in lower doses (Duran et al 2016). Silver nanoparticles have two pathways of toxicity; toxicity is either due to the particle's penetration of the cell membrane and the subsequent release of silver ions (for nanoparticles that are 80 nm or less), or through the

AgNPs own interactions with the cell (for particles less than 10 nm) (Duran et al 2016).

However, the efficacy of AgNPs is not without its consequences. The widespread use of AgNPs has led to their release into the environment through pathways such as everyday aqueous exposure (washing, sweat) (Hedburg et al 2014), or through the waste from the manufacturing process. Once in the natural environment, these antibacterial agents can cause harm to organisms that are not their intended target such as fish and plants, and even humans (Choi et al 2010, Kim et al 2013, Cvjetko et al 2017).

Once in the environment, silver nanoparticles can undergo changes in response to the interaction with different factors such as pH, light exposure, nanoparticle coating, and exposure to electrolytes and other water constituents. Some of the transformations undergone by AgNPs in the environment include sorption to organic and inorganic substances, oxidative dissolution, re-reduction, chlorination, and aggregation (Liu and Jiang 2015). The transformation undergone by an AgNP will affect its final fate and determine the extent to which it will be toxic to organisms. Aggregation, for example, can reduce toxicity as it results in particles of larger diameter (Duran et al 2016, Maillard and Hartemann 2013). In addition, the process of aggregation usually means reduced dissolution and therefore, less Ag^{+} released (Liu and Jiang 2015). Finally, larger particles

from aggregation can settle out of aqueous environments (Liu and Jiang 2015), positively affecting some organisms (e.g. fish) and negatively affecting others (e.g. aquatic plants).

Aggregation kinetics studies can be used to determine the stability of a particle. In these studies, environmentally relevant electrolytes are introduced to nanoparticle solutions to find the critical coagulation concentration (CCC), or the concentration at which the particles move from a reaction-limited aggregation regime to a diffusion-limited aggregation regime, according to Derjaguin-Landau-Verwey-Overbeek (DLVO) theory. DLVO theory is the primary theory used to explain the aggregation of particles in solution. It assumes that a relatively thin layer of ions surrounds a particle due to its charge (Derjaguin, B.V. and Landau, L.D. 1941, Verwey, E.J.W. and Overbeek, J.T.G. 1948). This “counter ion layer”, or “double layer” causes repulsive forces between two similar particles in a solution (Derjaguin, B.V. and Landau, L.D. 1941, Verwey, E.J.W. and Overbeek, J.T.G. 1948). In addition to the repulsive electrostatic forces, Van der Waal forces cause attractive forces between the particles, but the repulsive forces dominate, making the particles “stable,” by keeping them from aggregating (Derjaguin, B.V. and Landau, L.D. 1941, Verwey, E.J.W. and Overbeek, J.T.G. 1948). When electrolytes are introduced into the system, they screen, or neutralize, the counter ion layer, reducing the repulsive forces and allowing aggregation to occur (Derjaguin, B.V. and Landau, L.D. 1941, Verwey, E.J.W.

and Overbeek, J.T.G. 1948). In the reaction-limited regime of aggregation, an increase in electrolyte concentration likewise increases the aggregation rate (Derjaguin, B.V. and Landau, L.D. 1941, Verwey, E.J.W. and Overbeek, J.T.G. 1948). In the diffusion-limited regime of aggregation, the electrolyte concentration is high enough that increases in electrolyte concentration do not affect the aggregation rate of the nanoparticles, and aggregation is left up to Brownian motion (Derjaguin, B.V. and Landau, L.D. 1941, Verwey, E.J.W. and Overbeek, J.T.G. 1948). The particles aggregate rapidly, and are referred to as “unstable” (Derjaguin, B.V. and Landau, L.D. 1941, Verwey, E.J.W. and Overbeek, J.T.G. 1948). The concentration at which the particles become unstable (move from the reaction-limited regime to the diffusion-limited regime) is the critical coagulation concentration (Derjaguin, B.V. and Landau, L.D. 1941, Verwey, E.J.W. and Overbeek, J.T.G. 1948).

A variety of environmental factors can shift the CCC, making the CCC a common measure of the stability of nanoparticles in the environment. For instance, the coating of a particle (e.g., Citrate, PVP) is one factor that influences the extent to which the particle is affected by the environment. Coatings usually stabilize AgNPs (high CCC), making them less likely to aggregate (El Badawy et al 2012). In addition, divalent electrolytes ($CaCl_2$) are known to have a lower CCC than monovalent electrolytes ($NaNO_3$ and NaCl) due to their higher valence. This is otherwise known as the Schulze-Hardy rule (Elimelech et al 1995). Finally, the

pH of the system can influence the stability of AgNPs. Electrostatically stabilized AgNPs, such as citrate-coated AgNPs, have been found to aggregate in more acidic environments (El Badawy A. 2010).

Many studies have been conducted on the interactions of AgNPs and their fate in the natural environment. However, most studies focus on the behavior of AgNPs of one size. Studies in the field of toxicology have shown that the toxicity of AgNPs increases as particle size decreases (Duran et al 2016, Maillard and Hartemann 2013). Due to the effect of size on toxicity, as well as the variety of sizes in the market, there are most likely multiple sizes of AgNPs in the natural environment at this time. Therefore, it may be important to compare the behavior of AgNPs of different sizes when in the natural environment. This research aimed to determine if there were significant differences in AgNP behavior with respect to initial particle diameter via aggregation studies. Since it has been shown that smaller AgNPs are more toxic (Duran 2016, Maillard and Hartemann 2013) and that smaller AgNPs dissolve to a greater extent than larger particles (Peretyazhko T.S. et al 2014), the extent to which size has an effect of the aggregation of AgNPs in the environment could affect their toxicity. It was hypothesized that in pH 7 solution, smaller citrate-coated AgNPs, being more toxic and reactive with decreases in size, would also be less stable (have a lower CCC) than larger citrate-coated AgNPs in the presence of electrolytes ($NaNO_3$, NaCl, or $CaCl_2$).

2. Methods

2.1 Materials

Citrate-coated silver nanoparticles suspended in 2mM sodium citrate of nominal diameters 20 nm, 50 nm, and 80 nm (“NanoXact”) were purchased from nanoComposix. All other reagents were analytical grade or better. A buffer solution of 5.0×10^{-2} mM $NaHCO_3$ was prepared using deionized water (Milli-Q, Millipore) for a solution pH of 7.10 ± 0.06. Electrolyte solutions were prepared using the buffer solution to keep them at a pH of 7. All solutions were filtered through 0.1 um cellulose ester membranes (Millipore) before use. The silver nanoparticles were dialyzed in deionized water for 24 hours using Spectra/Por Biotech CE dialysis membranes (MWCO: 8-10 kD), with the deionized water being changed four times during this time period. The particles were dialyzed to remove excess sodium citrate. Before and after dialysis, the particles were characterized using a Brookhaven Dynamic Light Scattering (DLS) instrument (90Plus, Brookhaven Instruments Corp., Holtsville, NY), and a Shimazdu UV-4201PC UV-vis spectrophotometer over a wavelength of 200 – 700 nm. All labware and glassware were thoroughly cleaned before use with 10% nitric acid, followed by a thorough rinse with deionized water. Labware was subsequently air-dried under dust-free conditions.

2.2 Experiment

Experimental methods were based on those used by Li et al (2010). For the aggregation experiments, the stock silver nanoparticles were diluted in the 5.0 x 10^{-2} mM $NaHCO_3$ buffer at pH 7. However, the dilution factors differed between particle sizes, due to the difficulty of acquiring accurate measurements as the particle size decreased. Therefore, the 80 nm particles were diluted 10 times, the 50 nm particles were diluted 10 times, and the 20 nm particles were diluted 3 times.

Next, 3 mL of the nanoparticle solution was placed into a disposable acrylic cuvette, which had previously been rinsed with deionized water to minimize dust interference. After the addition of the nanoparticle solution, a pre-calculated amount of electrolyte solution was placed into the cuvette in order to obtain the target electrolyte concentration in the electrolyte-nanoparticle solution. Then the cuvette was capped with a plastic lid and hand-shaken for a few seconds before being inserted into the Dynamic Light Scattering (DLS) instrument. Measurements were taken promptly after the insertion of the sample, over periods of time ranging from 1 min and 40 s at a time interval of 10 s, to 15 min at a time interval of 90 s. All aggregation experiments were conducted at a temperature of 22 degree Celsius.

2.3 Aggregation Kinetics

The change in nanoparticle hydrodynamic diameter over time was measured using the DLS, and plotted in Exel (supporting information). The aggregation rate constant, k_{exp}, was obtained using Excel's linear regression function to derive a trend-line for the data series. In making the trend-line, only the data points recorded before an increase of 30% of the initial hydrodynamic diameter reading were used. This ensures that kinetics were only based on the aggregation of monomer AgNPs as opposed to dimer AgNPs (Chen et al 2006). The derivation of k_{exp} is based on the following expression (Virden et al 1992):

$$k_{exp} = \frac{1}{aNr_0}\frac{dr}{dt} \quad (1)$$

This expression shows the dependency of the aggregation rate on N, the initial particle concentration, r_0, the initial particle radius, and α, which is an optical factor. Next, the inverse stability ratio, "1/W," was calculated using the following equation (Virden et al 1992):

$$\frac{1}{W} = \frac{k_{exp}}{k_{fast}} \quad (2)$$

The value for k_{fast} was determined by taking the average of the two to three fastest k_{exp} values.

The CCC was determined by first drawing a trend-line through the steeply-sloped portion of the 1/W versus electrolyte concentration graph (the reaction-limited regime), and then a trend-line through the plateau area of the graph (the diffusion-limited regime). The electrolyte concentration at which the two trend-lines intersected was the CCC.

3. Results

3.1 Characterization of Silver Nanoparticles

A summary of the characteristics of the AgNPs used in this study are presented in Table 1. NanoComposix reported the particles to have hydrodynamic diameters of 25 nm for the 20 nm particles, 51 nm for the 50 nm particles, and 80 nm for the 80 nm particles (Table 1). The lab-measured hydrodynamic diameters of the stock 20 nm, 50 nm, and 80 nm particles after dialysis were 28.9 ± 0.7 nm, 52.5 ± 0.6 nm, and 81.6 ± 0.3 nm, respectively (Table 1). The nanoparticle solutions were noted to have a golden-yellow color before and after dialysis. The particles purchased from nanoComposix were reported to have a total silver concentration of 20 mg/mL. The AgNPs from Li et al, (2010) whose methods on which this work's methods were based on, synthesized bare AgNPs with a total silver concentration of 31.6 mg/L and used a dilution of 25 times for their analyses of bare AgNP interaction with electrolytes (Table 1). Using a dilution of 25 times for the purchased nanoparticles was not sufficient to gain accurate

readings from the DLS, as the total silver concentrations differed (Table 1). As a result, the dilution factor had to be decreased from 25 times to 10 times for the 80 nm and 50 nm particles. At 20 nm, accurate readings were still difficult to obtain with the DLS and low average count rates were observed, even though the total silver concentration was reported to be similar to the total silver concentrations of the 50 and 80 nm particles. In order to produce accurate DLS measurements for the 20 nm particles, the dilution factor dropped from 25 times to 3.3 times. UV-vis absorbance results, however, indicated the opposite trend in concentration, as the peak absorbance value for the 20 nm particles was much higher than that for the 50 and 80 nm particles (Figure 1). Since further analysis was unable to be conducted on the total silver concentration of the nanoparticle solutions, the low count rate in the DLS for the 20 nm particles was attributed to the inability of smaller particles to scatter light as efficiently as larger particles.

***Table 1**: Characteristics of AgNPs*

Entity	Size (nm)	Hydrodynamic Diameter (nm)	UV – peak wavelength (nm)	Total Ag Concentration (mg/L)	Dilution Factor used
nanoComposix Product Information	20 50 80	25 51 80	392 424 454	22 21 21	- - -
AgNP Lab Measurements (after dialysis in DI water)	20 50 80	28.0 ± 0.7 52.5 ± 0.6 81.6 ± 0.3	394 423 458	- - -	10 x 10 x 3.3 x
Li et al (2010) (bare AgNPs)	- - 80	- - 82.0 ± 1.3	- - 446	- - 31.6	- - 25 x

NanoComposix reported the particles to have a UV-vis peak of 392 nm for the 20 nm particles, 424 nm for the 50 nm particles, and 454 nm for the 80 nm particles. The UV-vis absorption spectrum (Figure 1) of the AgNP suspensions after dialysis showed a maximum absorption peak at a wavelength of 394.00 nm, 423.00 nm, and 458.00 for the 20 nm, 50 nm, and 80 nm particles, respectively. The close agreement between the stock and post-dialysis AgNP UV peaks, as well as between the stock and post-dialysis hydrodynamic diameters indicates that the dialysis process did not alter the nanoparticle properties.

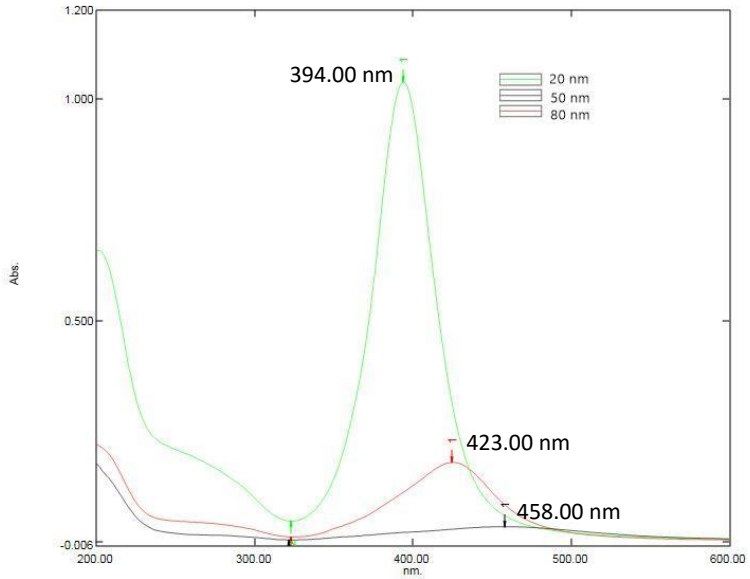

***Figure 1**: UV-vis peaks for stock 20, 50 and 80 nm AgNPs after dialysis*

3.2 Aggregation and Dissolution of Silver Nanoparticles in Sodium Nitrate

3.2.1 Aggregation and Dissolution of 20 nm Silver Nanoparticles in Sodium Nitrate

The aggregation rates of the 20 nm AgNPs in the presence of sodium nitrate exhibited behavior consistent with DLVO theory and are shown in Figure 2. At low concentrations of $NaNO_3$ (10 mM – 20 mM), the electrolytes were unable to screen the negative charge of the citrate-coated AgNP, and thus aggregation did not occur (supporting information). Between 30 mM and 50 mM, an increase in electrolyte concentration resulted in an increase in k_{exp}, consistent with the reaction-limited regime behavior. From 100 mM to 400 mM, the k_{exp} slightly decreased but did not increase, indicating the diffusion-limited regime. The plot of 1/W and $NaNO_3$ concentration showed the CCC of the 20 nm particles in $NaNO_3$ to be 50 mM (Figure 2).

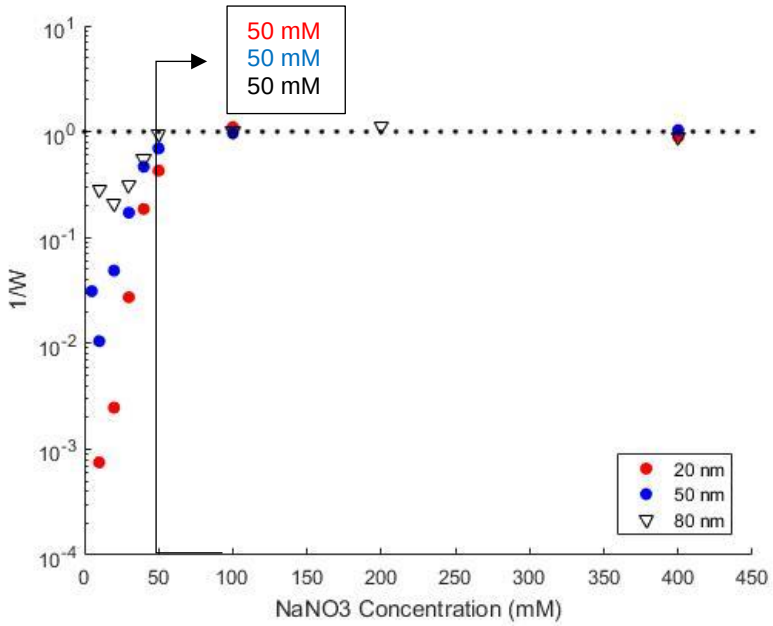

Figure 2: Stability of 20, 50 and 80 nm AgNPs in $NaNO_3$

Some initial dissolution was observed for the 20 nm AgNPs with the addition of $NaNO_3$. The backwards extrapolation of the trendline derived from the linear regression of hydrodynamic diameter over time for the 20 nm particles in $NaNO_3$ was used to determine the initial hydrodynamic diameter after the addition of $NaNO_3$ (supporting information). Values lower than the initial hydrodynamic diameter measured with the DLS in the absence of electrolytes for the 20 nm AgNPs (28.0 nm) indicated dissolution in the presence of the electrolyte (Figure 3). Initial dissolution occurred for low concentrations of NaNO3 (Figure 3). Past 30 mM, it seems that aggregation occurred too rapidly to be captured by the DLS, as the calculated initial hydrodynamic diameter was larger than the

hydrodynamic diameter measured with the DLS without any electrolytes (Figure 3).

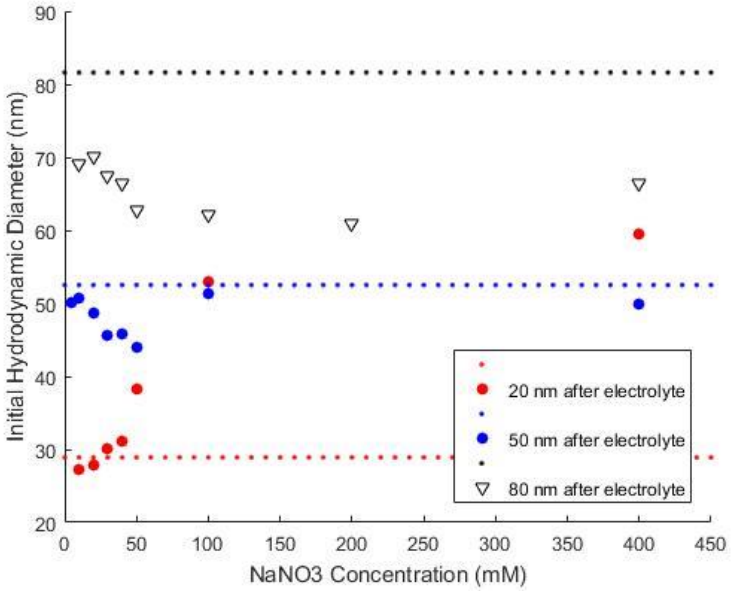

Figure 3: Initial Dissolution of 20, 50 and 80 nm AgNPs in $NaNO_3$ [1]

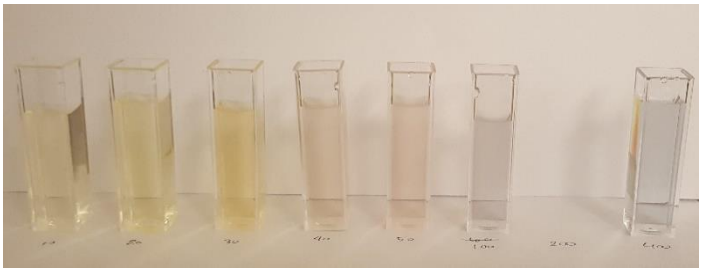

Figure 4*: 20 nm AgNPs after the addition of NaNO3*[2]

[1] Each dotted line indicates the initial AgNP hydrodynamic diameter before the addition of electrolytes; black is for the 80 nm AgNPs, blue is for the 50 nm AgNPs, and red is for the 20 nm AgNPs.

[2] Sodium nitrate concentration added, from left to right: 10 mM, 20 mM, 30 mM, 40 mM, 50 mM, 100 mM, 400 mM

As shown in Figure 4, a noticeable color change was evident with the addition of $NaNO_3$ to the 20 nm AgNPs. The initial color of the AgNPs before the addition of electrolytes was a pale golden-yellow. With the addition of 30 mM of $NaNO_3$, this color deepened after the conclusion of measurements for that sample. At 40 mM of $NaNO_3$ added, the solution was a dull purple color after the conclusion of measurements on that sample (10 min) (Figure 4). At 50 mM of $NaNO_3$ added, the solution changed almost instantly from yellow to pink (Figure 4). At 100 and 400 mM of $NaNO_3$ added, the solution instantly turned from yellow to purple-blue, and grey, respectively (Figure 4). It should be noted that the solutions remained clear with the color change, and did not turn cloudy. The initial hydrodynamic diameter after addition of $NaNO_3$ followed a similar pattern, with more aggregation occurring at higher concentrations of sodium nitrate (Figure 3), suggesting a correlation.

3.2.2 Aggregation and Dissolution of 50 nm Silver Nanoparticles in Sodium Nitrate

The aggregation rates of the 50 nm AgNPs in the presence of sodium nitrate also exhibited DLVO theory behavior. At low concentrations of $NaNO_3$ (10 mM – 20 mM), the addition of $NaNO_3$ only aggregated the particles enough to overcome the initial dissolution (supporting information). Between 30 mM and 50 mM, an increase in electrolyte concentration resulted in an increase in k_{exp} (Figure 2). From 100 mM to 400 mM, the aggregation rate barely increased, indicating the

diffusion-limited regime (Figure 2). The plot of 1/W and $NaNO_3$ concentration showed the CCC of the 50 nm particles in $NaNO_3$ to be 50 mM (Figure 2). Unlike with the 20 nm AgNPs, there appeared to be some initial dissolution of the 50 nm particles for all concentrations of $NaNO_3$ (Figure 3)

3.2.3 Aggregation and Dissolution of 80 nm Silver Nanoparticles in Sodium Nitrate

As with the 20 and 50 nm AgNPs, the aggregation rates of the 80 nm AgNPs in the presence of sodium nitrate also exhibited DLVO – theory behavior. At low concentrations of $NaNO_3$ (10 mM – 20 mM), the addition of $NaNO_3$ only aggregated the particles enough to overcome the observed initial dissolution (supporting information). Between 30 mM and 50 mM, an increase in electrolyte concentration resulted in an increase in k_{exp} (Figure 2). From 100 mM to 400 mM, the aggregation rate barely increased, indicating the diffusion-limited regime (Figure 2). The plot of 1/W and $NaNO_3$ concentration showed the CCC of the 80 nm particles in $NaNO_3$ to be 50 mM (Figure 2). As with the 50 nm AgNPs, there appeared to be initial dissolution of the 80 nm AgNPs for all concentrations of $NaNO_3$, however, the 80 nm particles dissolved to a greater extent at higher concentrations (Figure 3).

3.3 Aggregation and Dissolution of Silver Nanoparticles in Sodium Chloride

3.3.1 Aggregation and Dissolution of 20 nm Silver Nanoparticles in Sodium Chloride

The 20 nm AgNPs exhibited DLVO behavior in the presence of NaCl. At low concentrations (10, 20 and 30 mM), the particles aggregated only enough to return to the initial hydrodynamic diameter observed before the addition of NaCl (supporting information). From concentrations of 40 mM to 50 mM, the aggregation rate increased with increase in NaCl concentration (Figure 5). This trend peaked at 100 mM NaCl, and then for higher concentrations (200 mM and 400 mM), the aggregation rate was lower than observed at 100 mM (Figure 5). The plot of 1/W and NaCl concentration showed the CCC of the 20 nm particles to be 60 mM (Figure 5). Initial dissolution with the addition of NaCl was observed for the 20 nm AgNPs between 10 and 200 mM, with initial aggregation too rapid to be captured by the DLS occurring at 400 mM NaCl (Figure 6).

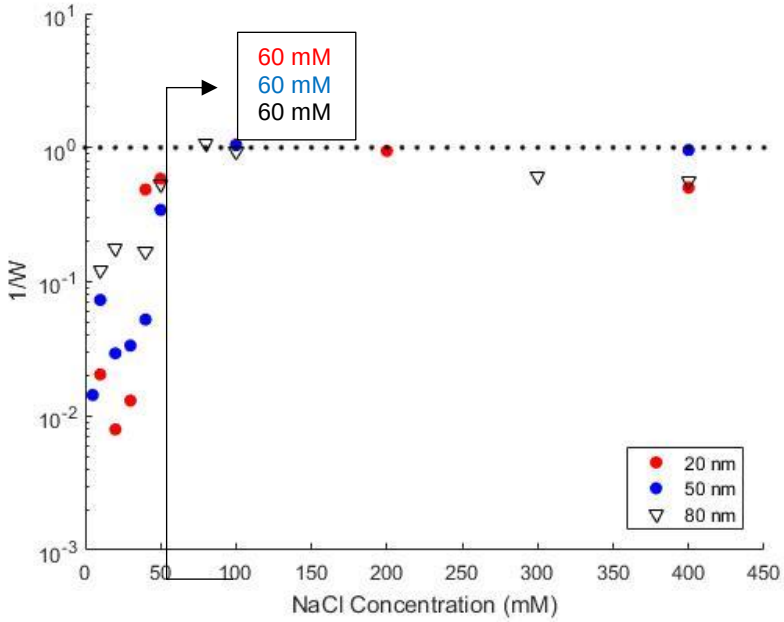

***Figure 5**: Stability of 20, 50 and 80 nm AgNPs in NaCl*

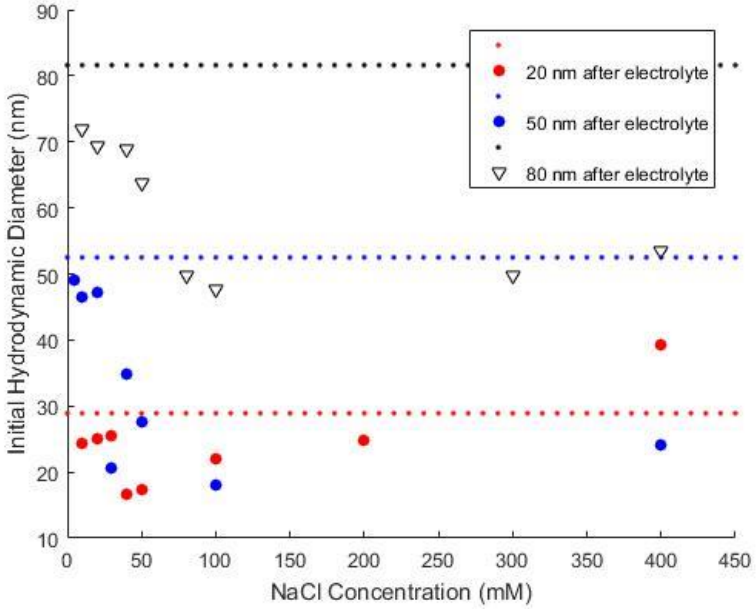

***Figure 6**: Initial Dissolution of 20, 50 and 80 nm AgNPs in NaCl*[3]

[3] Each dotted line indicates the initial AgNP hydrodynamic diameter before the addition of electrolyes; black is for the 80 nm AgNPs, blue is for the 50 nm AgNPs, and red is for the 20 nm AgNPs

3.3.2 Aggregation and Dissolution of 50 nm Silver Nanoparticles in Sodium Chloride

The 50 nm AgNPs also exhibited DLVO behavior in the presence of NaCl. At low concentrations (5, 10, 20 and 30 mM), little aggregation was observed with an increase in NaCl concentration (supporting information). Reaction-limited aggregation was observed between the concentrations of 40 and 50 mM (Figure 5). At 100 and 400 mM, aggregation followed diffusion-limited behavior, as the aggregation rate changed very little between those concentrations (Figure 5). The plot of 1/W and NaCl concentration showed that the CCC of the 50 nm particles was 60 mM (Figure 5).

Initial dissolution with the addition of NaCl was very apparent for the 50 nm AgNPs (Figure 6). This was especially important at the concentrations of 30 mM and 40 mM. At these concentrations the hydrodynamic diameter dropped to around 20 nm at 30 mM, and 35 nm at 40 mM (supporting information). While at other concentrations this initial dissolution was overcome and aggregation proceeded past the initial hydrodynamic diameter of the particles without electrolytes (52.5 nm), at 30 and 40 mM the AgNPs never aggregated enough to overcome the initial dissolution (supporting information). This did not seem to drastically affect the CCC.

3.3.3 Aggregation and Dissolution of 80 nm Silver Nanoparticles in Sodium Chloride

As with the 20 and 50 nm AgNPs, the 80 nm AgNPs exhibited DLVO behavior in the presence of NaCl. At low concentrations of electrolyte (10, 20 and 40 mM), little aggregation was observed with an increase in NaCl concentration (supporting information). Between 50 and 80 mM NaCl, reaction-limited aggregation behavior was observed (Figure 5). A decrease in aggregation rate was observed after 80 mM for high concentrations (100, 300 and 400 mM) (Figure 5). The plot of 1/W and NaCl concentration showed that the CCC of the 80 nm particles was 60 mM (Figure 5). Initial dissolution with the addition of NaCl was also observed for the 80 nm AgNPs at all concentrations of NaCl (Figure 6), and at a greater extent than observed for the 80 nm particles in $NaNO_3$ (Figure 3).

3.4 Aggregation and Dissolution of Silver Nanoparticles in Calcium Chloride

3.4.1 Aggregation and Dissolution of 20 nm Silver Nanoparticles in Calcium Chloride

The 20 nm AgNPs exhibited DLVO behavior in the presence of $CaCl_2$. At low concentrations of $CaCl_2$ (0.5 and 1 mM), particle size stayed relatively constant (supporting information). At 3 mM, the aggregation rate increased, and between 5 mM and 12 mM, the change in aggregation rate started to plateau (Figure 7).

However, more data points could have been collected at concentrations above 12 mM to make sure this was the case. The plot of 1/W and $CaCl_2$ showed that the CCC of the 20 nm particles was 3 mM (Figure 7).

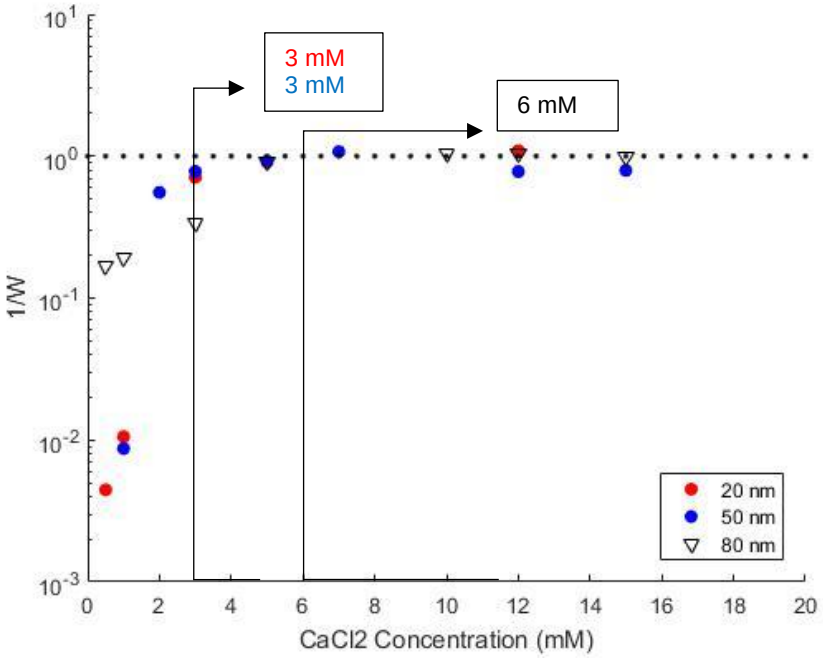

***Figure 7**: Stability of 20, 50 and 80 nm AgNPs in $CaCl_2$*

In addition, the electrolyte $CaCl_2$ exhibited typical Schulze-Hardy behavior as a divalent cation. Divalent cations are known to better neutralize surface charge at lower concentrations than monovalent cations, which is why the CCC is at a much lower concentration for $CaCl_2$ than for $NaNO_3$ and NaCl (Elimelech et al 1995).

As observed with $NaNO_3$ and NaCl, initial dissolution occurred after the addition of $CaCl_2$ for the 20 nm AgNP particles. In this case, all concentrations added (0.5 mM to 12 mM) caused dissolution, and no exceedingly rapid aggregation was observed (Figure 8).

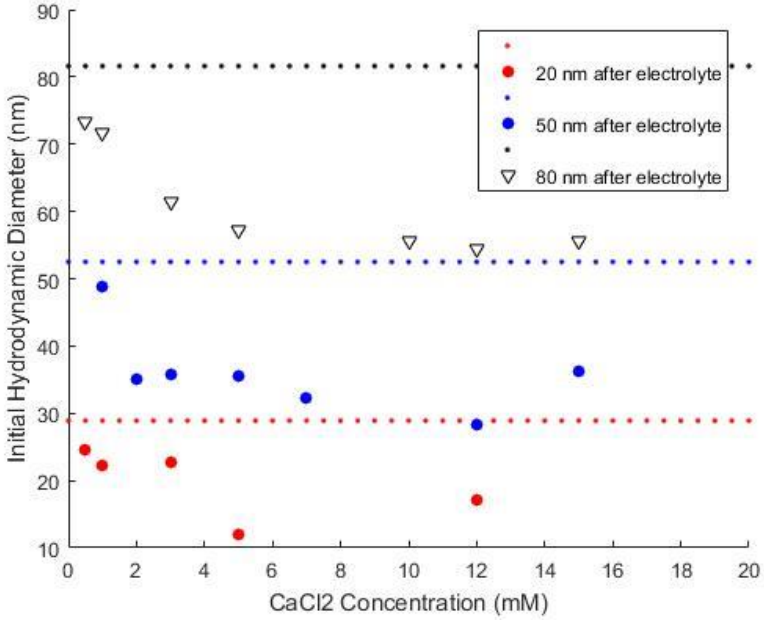

Figure 8: *Initial Dissolution of 20, 50 and 80 nm AgNPs in* $CaCl_2$[4]

[4] Each dotted line indicates the initial AgNP hydrodynamic diameter before the addition of electrolytes; black is for the 80 nm AgNPs, blue is for the 50 nm AgNPs, and red is for the 20 nm AgNPs

3.4.2 Aggregation and Dissolution of 50 nm Silver Nanoparticles in Calcium Chloride

The 50 nm AgNPs exhibited DLVO behavior in the presence of $CaCl_2$ as well. At 1 mM $CaCl_2$, no aggregation was observed (supporting information). For the concentrations of 2, 3, and 5 mM, the aggregation rate increased with concentration (Figure 7). At 7 mM, the aggregation rate reached a peak and started to decline for higher concentrations (12 and 15 mM) (Figure 7). The plot of 1/W and $CaCl_2$ concentration showed the CCC of the 50 nm particles to be 3 mM (Figure 7). As with the 20 nm AgNPs, initial dissolution was observed for the 50 nm AgNPs for all concentrations (1 – 15 mM) of $CaCl_2$ (Figure 8). The initial dissolution with $CaCl_2$ was less dramatic than the dissolution of the 50 nm particles in NaCl (Figure 6)

3.4.3 Aggregation and Dissolution of 80 nm Silver Nanoparticles in Calcium Chloride

As with the 20 and 50 nm AgNPs, the 80 nm AgNPs exhibited DLVO behavior in the presence of $CaCl_2$. For low concentrations (0.5 and 1 mM), little to no aggregation was observed, except for that used to overcome a slight initial dissolution after the addition of $CaCl_2$ (supporting information). For subsequent concentrations (3 and 5 mM), the aggregation rate increased with $CaCl_2$ concentration (Figure 7). Past 5 mM (10, 12 and 15 mM), the aggregation rate changed very little with increase in $CaCl_2$ concentration (Figure 7). The plot of

1/W and $CaCl_2$ concentration showed the CCC of the 80 nm particles to be 6 mM (Figure 7). As with the 50 and 20 nm particles, initial dissolution of the 80 nm AgNPs with the addition of $CaCl_2$ was observed for all concentrations of $CaCl_2$ added (Figure 8). This dissolution was less than the dissolution observed for the 80 nm particles in NaCl (Figure 6).

4. Discussion

4.1 Critical Coagulation Concentration Trends for $NaNO_3$ and NaCl

The hypothesis of this experiment was that the CCC for all electrolyte types would decrease for each decrease in size of AgNPs. This was not the case for $NaNO_3$ and NaCl, as their CCCs were size-independent (Table 2). While the original hypothesis was based on the reactivity of AgNPs in regards to dissolution, and not DLVO theory, there is still some discrepancy with the behavior of the particles as predicted by DLVO theory.

Table 2: CCC Values for 20, 50 and 80 nm AgNPs

AgNP size (nm)	$NaNO_3$ CCC (mM)	NaCl CCC (mM)	$CaCl_2$ CCC (mM)
20 nm	50	60	3
50 nm	50	60	3
80 nm	50	60	6

According to the original DLVO theory, with indifferent electrolytes, such as calcium and sodium, particle size and concentration have no effect on the CCC

(Elimelech et al 1995). This can be attributed to an assumption made in the theory that the counter ion layer is much smaller than the particle size (Afshinnia et al 2017). However, this part of the theory has been questioned in recent years.

The Fuchs approach to DLVO theory indicates a theoretical influence of particle size on the CCC (Elimelech et al 1995). However, Elimelech et al (1995) also noted that past studies have failed to observe this appreciable dependence on size. While few to no studies for the exclusive effect of AgNP size on CCC currently exist, Afshinnia et al (2017) conducted a review of different aggregation kinetics studies on AgNPs using different factors in AgNP aggregation kinetics, including size. They concluded that for monovalent electrolytes, while the aggregation rate during the reaction-limited regime of aggregation increased with an increase in size, the CCC increased with a decrease in AgNP size (Afshinnia et al 2017). This observation was supported by work conducted by Hsu and Liu, who determined that the assumption of relative counter ion layer size made in DLVO theory will only hold true for large particles with a radius of 1 um or larger (Hsu and Liu 1998). For particles smaller than 1 um, DLVO theory will underestimate the CCC (Hsu and Liu 1998). In addition, they noted that larger surface charges exacerbated the deviation from DLVO theory (Hsu and Liu 1998). The particles used in this experiment were all smaller than 1 um, and therefore subject to the deviation trend predicted by Hsu and Liu.

Afshinnia et al also noted that other studies conducted with nanoparticles other than silver observed varying trends between particle size and CCC. For hematite and TiO_2 nanoparticles the CCC decreased with a decrease in size, for CdSe nanoparticles the CCC increased with a decrease in size, and for AuNPs the CCC was independent of CCC (Afshinnia et al 2017). Thus, while it appears that the CCC should be size-dependent, and smaller particles should be more stable than larger particles, observing behavior contrary to the theory for the CCC is not unusual. Deviances between trends could be due to differences in experimental conditions such as particle concentration, surface charge, and particle-surface characteristics. It was noted in the methods section that the particle concentrations in this experiment were very different between the 50, 80 nm particles and the 20 nm particles, so this may have influenced the results in some way. Overall, however, the CCC values observed for the AgNPs in NaCl (60 mM), fall within the range of 40 – 70 mM that has been observed in the literature (Baalousha et al 2013). This provides some confirmation for the methods used and the CCCs observed.

Initial dissolution was observed for the AgNPs after the addition of electrolytes. This behavior is consistent with what has been observed in other studies (Li et al 2010, Baalousha 2013). It is most likely due to oxidative dissolution, which occurs when the equilibrium between Ag^+ ions adsorbed to the particle and in solution is disrupted by the introduced electrolyte (Li et al 2010). The Ag^+ ions

normally prevent oxidative dissolution, but when the equilibrium is disrupted they are displaced, and dissolution can occur (Li et al 2010).

A color change was observed for the 20 nm AgNPs in the presence of sodium nitrate. While the explanation of this result is out of the scope of this research, it is worth noting that Zhou et al (2016) observed a unique behavior of silver nanoparticles in sodium nitrate as well. In the presence of sodium nitrate, the AgNPs experienced drastic aggregation (70 to 700 nm) within a period of two days (Zhou et al 2016). Further TEM analysis showed evidence of a change in morphology and the formation of crystalline structures, but the mechanism of this change was unexplained (Zhou et al 2016). The 20 nm experiments were the last conducted of the three sizes. Therefore, while this trend may have occurred for the other sizes with $NaNO_3$, it was not observed. Further study on the nature of the interactions between silver and sodium nitrate should be conducted.

4.2 Critical Coagulation Concentration Trend for $CaCl_2$

For $CaCl_2$, the CCC increased with an increase in AgNP size (Table 2). While this result was in line with the initial hypothesis, the deviation from the $NaNO_3$ and NaCl results brought these results into question. While the Schulze-Hardy rule explains the efficiency of divalent cations in aggregating nanoparticles as opposed to monovalent cations, it does not necessarily explain the opposite

trend with respect to size of the nanoparticles. In addition, Afshinnia et al noted no observance of trend across studies between AgNP size and CCC for divalent cations (2017). It could be that three particle sizes were not enough data points to see an absence of a trend, or it could be that other forces dominated the reactions of $CaCl_2$ with the 20, 50 and 80 nm AgNPs, resulting in a positive trend between the CCC and AgNP size. Overall, since the CCC values for the 20 and 50 nm AgNPs (3 mM) fall near the CCC values of ~2 mM observed in other studies (Baalousha 2013), the 80 nm CCC of 6 mM seems high. Given that the CCC was size-independent for the monovalent cations, that the CCC for the 20 and 50 nm particles in $CaCl_2$ were the same, and that the 80 nm CCC was unusually high, the 80 nm CCC may have been influenced by experimental error.

5. Conclusion

Silver nanoparticles are a useful antibacterial agent as their size makes them more efficient. However, the popularity of these materials has led to their release into the environment, where they have the potential to harm non-target organisms. Several reactions can influence the fate and toxicity of AgNPs in the environment, including aggregation. Aggregation kinetics studies were conducted using the electrolytes $NaNO_3$, NaCl, and $CaCl_2$ on citrate-coated AgNPs of sizes 20, 50 and 80 nm at a pH of 7. Size-independent behavior was noted for all sizes of AgNPs in $NaNO_3$ and NaCl. In $CaCl_2$, larger particles were more stable (the

CCC increased with an increase in AgNP size). While the differences between expected and observed trends for $NaNO_3$ and NaCl could be attributed to differences between DLVO theory and actual experiment conditions, further research exclusively focused on the effect of AgNP size on stability should be conducted for both monovalent and divalent electrolytes.

6. References

Afshinnia K.; et al. Effect of nanomaterial and media physiochemical properties on Ag NM aggregation kinetics. *Journal of Colloid and Interface Science*, 2017; 487: 192-200.

Baalousha M.; et al. Effect of monovalent and divalent cations, anions and fulvic acid on aggregation of citrate-coated silver nanoparticles. *Science of the Total Environment*, 2013; 454-455: 119-131.

Chen K.L.; et al. Aggregation Kinetics of Alginate-Coated Hematite Nanoparticles in Monovalent and Divalent Electrolytes. *Environmental Science and Technology,* 2006; 40: 1516-1523.

Choi J. E.; et al. Induction of oxidative stress and apoptosis by silver nanoparticles in the liver of adult zebrafish. *Aquatic Toxicology*, 2010; 100: 151-159.

Cvjetko P.; et al. Toxicity of silver ions and differently coated silver nanoparticles in Allium cepa roots. *Ecotoxicology and Environmental Safety*, 2017; 137: 18-28.

Derjaguin, B. V.; Landau, L. D. Acta Physicochim. 1941, 14, 733.

Duran N.; et al. Silver nanoparticles: A new view on mechanistic aspects on antimicrobial activity. *Nanomedicine: Nanotechnology, Biology, and Medicine*, 2016; 12: 789-799.

El Badawy A. M.; et al. The impact of stabilization mechanism on the aggregation kinetics of silver nanoparticles. *Science of the Total Environment*, 2012; 429: 325-331.

El Badawy A. M.; et al. Impact of Environmental Conditions (pH, Ionic Strength, and Electrolyte Type) on the Surface Charge and Aggregation of Silver Nanoparticle Suspensions. *Environmental Science and Technology*, 2010; 44: 1260-1266.

Elimelech M., et al. Particle Deposition and Aggregation: Measurement, Modeling and Simulation. Oxford: Butterworth-Heinemann Ltd.. 1995.

Hedburg J.; et al. Sequential Studies of Silver Released from Silver nanoparticles in Aqueous Media Simulating Seat, laundry Detergent Solutions and Surface water. *Environmental Science and Technology*, 2014; 48: 7314-7322.

Hsu, Jyh-Ping and Liu, Bo-Tau. Effect of Particle Size on Critical Coagulation Concentration. *Journal of Colloid and Interface Science*, 1998; 198: 186-189.

Kim J. Y.; et al. Developmental toxicity of *Japanese medaka* embryos by silver nanoparticles and released ions in the presence of humic acid. *Ecotoxicology and Environmental Safety*, 2013; 92: 57-63.

Liu J and Jiang G (editors). Silver Nanoparticles in the Environment. Heidelberg: Springer. 2015.

Li X.; et al. Dissolution-Accompanied Aggregation Kinetics of Silver Nanoparticles. *Langmuir*, 2010; 26(22): 16690-16698.

Maillard, Jean-Yves, Hartemann P. Silver as an antimicrobial: facts and gaps in knowledge. *Critical Reviews in Microbiology*, 2013; 39(4): 373-383.

Peretyazhko T.S.; et al. Size-Controlled Dissolution of Silver Nanoparticles at Neutral and Acidic pH Conditions: Kinetics and Size Changes. *Environmental Science and Technology,* 2014; 48: 11954-11961.

Verwey, E. J. W.; Overbeek, J. T. G. Theory of the Stability of Lyophobic Colloids; Elsevier: Amsterdam, 1948.

Virden, J. W.; Berg, J. C. J. *Colloid Interface Sci*., 1992; 149: 528.

Zhou W.; et al. Effects of pH, Electrolyte, Humic Acid, and Light Exposure on the Long-Term Fate of Silver Nanoparticles. *Environmental Science & Technology*, 2016; (web).

Zodrow K.; et al. Polysulfone ultrafiltration membranes impregnated with silver nanoparticles show improved biofouling resistance and virus removal. *Water Research*, 2009; 43: 715-723.

Supporting Information

Raw Data: DLS Readings for 20, 50 and 80 nm AgNPs, k_{exp} values, k_{fast} values

***Table 3**: Stock AgNP DLS measurements*

AgNP size	Effective Diameter (nm)	Standard Deviation	Half-Width (nm)	Standard Deviation	Polydispersity	Standard Deviation	Sample Quality	Standard Deviation	Average Count Rate (kcps)	UV peak wavelength (nm)	Absorbance
80 nm	81.6	0.3	29.3	0.8	0.129	0.007	8.8	0.3	185.0	458.00	0.035
50 nm	52.5	0.6	17.1	0.5	0.108	0.006	7.2	0.4	29.7	425.00	0.180
20 nm	28.5	0.5	11.3	3.0	0.166	0.071	0	0	9.3	394.00	1.039

Note: these are post-dialysis measurements

***Table 4:** Aggregation kinetics data for 80 nm AgNPs*

				Average Size per run (nm)												
nAg stock size (nm)	Electrolyte Type	Electrolye Conc. (mM)	Run Length (min)	1	2	3	4	5	6	7	8	9	10			
				1.5	3	4.5	6	7.5	9	10.5	12	13.5	15	K_exp	K_fast	α
80	NaNO3	10	1.5	69.8	73.8	75.1	75.5	77.8	77.8	77.9	77.2	77.1	77.5	1.18	4.13	0.286
		20		69.4	72.5	75.2	77.9	77.4	77.9	78.8	79.5	78.8	79.5	0.871	4.13	0.211
		30		67.8	71.9	75	75.9	76.7	78.5	77.4	78.6	79.1	78.3	1.31	4.13	0.317
		40		68.6	73.5	76.7	82	84.1	86.3	89.6	89.8	93.4	93.8	2.29	4.13	0.554
		50		68.3	75.3	80.1	85.5	92.3	93	96.8	97.1	100.4	103.8	3.88	4.13	0.940
		100		68	75	82.6	87.1	93.7	95.8	102.2	105.7	110.6	111.4	4.23	4.13	1.03
		200		67.5	76	81.4	89.1	92.6	97	100.3	102.7	106.7	109.3	4.68	4.13	1.13
		400		72	77	83.2	90	93.4	98.6	101	107	109.9	112.8	3.72	4.13	0.901
				1.5	3	4.5	6	7.5	9	10.5	12	13.5	15	K_exp	K_fast	α
80	CaCl2	0.5	1.5	69.1	76.5	79.3	78.1	79.8	78.8	79.7	79.5	79.3	82.4	0.582	3.43	0.170
		1		70	73.8	75.4	77.1	78	78	79.3	79.7	79.4	80.7	0.66	3.43	0.193
		3		63.3	64.5	65.4	68.3	71.9	73.1	72.7	75.6	76.6	78.7	1.17	3.43	0.340
		5		61.9	67	71.2	76	78.6	86.5	88	91.5	96.1	98.3	3.10	3.43	0.904
		10		61.1	65.7	72.3	77.4	82.2	91.2	92.2	96.7	99.3	104.2	3.59	3.43	1.05
		12		60.2	65.1	70.2	76.4	81.7	86.5	88.8	93.3	98.4	100.9	3.62	3.43	1.06
		15		61.3	64.7	71.2	76.3	81	85.7	91.7	95.9	99	102.8	3.40	3.43	0.992
				1.5	3	4.5	6	7.5	9	10.5	12	13.5	15	K_exp	K_fast	α
80	NaCl	10	1.5	72.1	74.3	75.7	76.4		77.6	78.9	77.7	78.3	79.1	0.674	5.60	0.120
		20		68.9	72.3	75.5	77.5	76.5	78.1	78.6	77.6	78.8	78	0.993	5.60	0.177
		40		67.2	71.8	75.2	74.9	77.7	78.1	80.3	80.2	81.1	81.2	0.940	5.60	0.168
		50		67.5	72.6	77.5	81.9	86.5	89.3	89.5	91.4	94.4	96.3	2.954	5.60	0.528
		80		58.9	67.5	76.9	84.9	93.3	98.2	103.2	107.1	112.6	115.6	6.00	5.60	1.07
		100		55.7	62.5	72	78.5	85.9	90.7	93.6	100.3	103.5	107.4	5.19	5.60	0.928
		300		56.1	59	64.8	70.2	76.2	80.6	83	88.5	97.7	96.8	3.43	5.60	0.612
		400		58.9	62.5	66.8	73.3	77	83.6	86.5	92	95.4	99.8	3.13	5.60	0.560

***Table 5**: Aggregation kinetics data for 50 nm AgNPs*

				Average Size per run (nm)												
nAg stock size (nm)	Electrolyte Type	Electrolye Conc. (mM)	Run Length (min)	1	2	3	4	5	6	7	8	9	10			
				1.5	**3**	**4.5**	**6**	**7.5**	**9**	**10.5**	**12**	**13.5**	**15**	**K_exp**	**K_fast**	**α**
50	NaNO3	5	1		51.7	50.1	52.5	50.7	50.3	52.6	52.1	53.5		0.179	5.74	0.0311
		10			48.8		54.4	50.8	51.2	51.8	50.2	51.8	51.4	0.060	5.74	0.0105
		20		50.3	49.8		49		50.2		50.8	52.1	54.9	0.280	5.74	0.0487
		30		46.8	49.1	50.3		54.5	53	55.9	56.9	60	58.1	0.986	5.74	0.172
		40		49.1	54	~~66.3~~	60.4	66	68.2	70.2	73	76	76.6	2.68	5.74	0.467
		50		49.9	55.7	61.8	67.8	72.6	75.9	81	84	87.6	92.3	3.99	5.74	0.694
		100		59	69.2	76	84.5	89.4	93.6	100.6	106.6	111.3	113.9	5.55	5.74	0.967
		400		58.2	68.7	76	82	92	95.6	102.4	106.3	112.1	121	5.93	5.74	1.03
				1.5	**3**	**4.5**	**6**	**7.5**	**9**	**10.5**	**12**	**13.5**	**15**	**K_exp**	**K_fast**	**α**
50	CaCl2	1	1.5	48.8	49.2	49.2	49.8	49.2	48.1	49	50.8	50.8	48.7	0.060	6.87	0.0087
		2		41.2	45.7	52.6	58	68.5	73.2	79.6	84.8	90.9	97.3	3.820	6.87	0.5560
		3		46.1	51.8	62.2	71.1	80.1	88.8	96.6	105.6	110.1	116.5	5.367	6.87	0.7812
				1	**2**	**3**	**4**	**5**	**6**	**7**	**8**	**9**	**10**			
		3.2	1	42.9	48.6	56.5	63.3	67.7	74.6	84.5	88.5	91.5	97.8	5.37	6.87	0.781
		5		42.9	46.8	54.4	61.5	66.6	75.2	81.9	84.8	91.8	95.5	6.34	6.87	0.923
				1.5	**3**	**4.5**	**6**	**7.5**	**9**	**10.5**	**12**	**13.5**	**15**			
		7	1.5	43.9	53.5	66.1	73.5	84.5	91	100.8	107.3	114.7	124.4	7.40	6.87	1.08
				1	**2**	**3**	**4**	**5**	**6**	**7**	**8**	**9**	**10**			
		12	1	34.3	37.6	45	53.6	59.9	68	70.6	77.9	83.3	92.1	5.35	6.87	0.78
		15		42.8	46.4	51.1	59.4	64.9	69.1	76.3	82.1	85.8	94	5.45	6.87	0.793304221
				1.5	**3**	**4.5**	**6**	**7.5**	**9**	**10.5**	**12**	**13.5**	**15**	**K_exp**	**K_fast**	**α**
50	NaCl	5	1	49	50	49.8	49.8	49.8	50.3	48.9	51.8	50.4	49.9	0.124	8.65	0.0143
		10		47.3	48.8	48.7	50.5	48.5	49.3	50.5	48.7	49.9	50.4	0.633	8.65	0.0732
		20		48.3	47.8	48.4	47.8	48.7	49.7	50.3	49.8	48.5	53	0.253	8.65	0.0293
		30			21.2	21.4	24.2	22	22.6	23.2	23.5		25.5	0.289	8.65	0.0335
		40		35	35.9	37.5	38	38.4	39.7	38.2	42.2	40.3	41.2	0.453	8.65	0.0523
			TIME:	**1**	**2**	**3**	**4**	**5**	**6**	**7**	**8**	**9**	**10**	**K_exp**	**K_fast**	**α**
		50	1.5	31	33.4	36.5	37.1	44	42.1	45.4	49.4	51.7	55.8	2.97	8.65	0.343
		100		27.7	34.6	45.7	54.8	62.1	72.4	78.9	88	94.6	99.1	9.00	8.65	1.04
		400		32.8	39.5	49.4	61	68.1	74.3	83.2	88.4	95.9	104	8.30	8.65	0.960

***Table 6**: Aggregation kinetics data for 20 nm AgNPs*

				Average Size per run (nm)												
nAg stock size (nm)	Electrolyte Type	Electrolye Conc. (mM)	Run Length (min)	1	2	3	4	5	6	7	8	9	10			
				1.5	**3**	**4.5**	**6**	**7.5**	**9**	**10.5**	**12**	**13.5**	**15**	**K_exp**	**K_fast**	**α**
20	NaNO3	10	1.5	27.3	27.7	28.5	27.1	27.6	26.9	28.4	28.3	27	30	0.0873	116.25	0.000751
		20		27.2	27.8	29.8		31.4	31.8	30.3	31.2	30.5	31.9	0.287	116.25	0.00247
				1	**2**	**3**	**4**	**5**	**6**	**7**	**8**	**9**	**10**			
		30	1	33.6	36	39.4	43.1	45.9	48.9	50.9	53.4	56.3	59.3	3.17	116.25	0.0273
				0.75	**1.5**	**2.25**	**3**	**3.75**	**4.5**	**5.25**	**6**	**6.75**	**7.5**			
		40	0.75	48	65.8	84	101.5	112.4	128.8	140.8	147.8	155.4	172.7	23.7	116.25	0.204
				0.33	**0.67**	**1.00**	**1.33**	**1.67**	**2.00**	**2.33**	**2.67**	**3.00**	**3.33**			
		40	0.33	38.4	47.2	52.8	60.5	68.6	72.5	82.2	89.7	95.6	107.1	21.6	116.25	0.186
		50		54.8	71.4	92.3	105.5	124.4	138.7	146.9	164.3	162.8	172	49.8	116.25	0.428
				0.17	**0.33**	**0.50**	**0.67**	**0.83**	**1.00**	**1.17**	**1.33**	**1.50**	**1.67**			
		100	0.17	75.3	93.8	118.1	131.1	145.8	152.1	162	170.3	168.8	180.3	128.4	116.25	1.10
		400		75.7	96.1	110.4	126.6	134.5	150.3	150.3	160.1	160.5	172.1	104.1	116.25	0.895
				1.5	**3**	**4.5**	**6**	**7.5**	**9**	**10.5**	**12**	**13.5**	**15**	**K_exp**	**K_fast**	**α**
20	CaCl2	0.5	1.5	25.1	27.4	27.1	28.7	26.7	27.3	27	27.6	27.6	28.4	0.118	26.4	0.00445
				0.5	**1**	**1.5**	**2**	**2.5**	**3**	**3.5**	**4**	**4.5**	**5**			
		1	0.5	22.5	22	22.3	22.3	21.5	22	25.8	21.9	24	22.5	0.279	26.4	0.0106
				0.5	**1**	**1.5**	**2**	**2.5**	**3**	**3.5**	**4**	**4.5**	**5**			
		3	0.5	37.4	52.1	60	69.1	82.1	89.3	99.5	106.1	114.4	124.5	18.8	26.4	0.711
				0.33	**0.67**	**1.00**	**1.33**	**1.67**	**2.00**	**2.33**	**2.67**	**3.00**	**3.33**			
		5	0.33	27.2	42.4	50.4	56.3	67.5	72.6	84.3	88	98	99.7	24.0	26.4	0.908
		12		28.7	40.2	50.7	60.2	72.2	78.9	84.3	92.5	93.7	106.9	28.8	26.4	1.09
				1.5	**3**	**4.5**	**6**	**7.5**	**9**	**10.5**	**12**	**13.5**	**15**	**K_exp**	**K_fast**	**α**
20	NaCl	10	1.5	25.6	25.5	26.6	26.1	27.2	28.6	27.6	29.6	30.6	30.7	0.414	20.3	0.0204
		20		25.2	24.9	26.8	26.4	26.1	26.6	26.4	27.8	27.5	27	0.161	20.3	0.00793
		30		25.8	26	26.6	27.3	27.4	27	28.3	28.9	28.8		0.264	20.3	0.0130
				0.5	**1**	**1.5**	**2**	**2.5**	**3**	**3.5**	**4**	**4.5**	**5**			
		40	0.5	20.9	26.4	30	37.9	41.6	45.9	50.9	56.4	62.4	66.2	9.90	20.3	0.487
				1.5	**3**	**4.5**	**6**	**7.5**	**9**	**10.5**	**12**	**13.5**	**15**			
		50	1.5	35.2	53.1	72.1	89.7	98.4	116.6	132.8	140.8	152.6	167.4	11.9	20.3	0.587
				0.33	**0.67**	**1.00**	**1.33**	**1.67**	**2.00**	**2.33**	**2.67**	**3.00**	**3.33**			
		100		29.8	35	44.1	53.2	60.8	67.7	73.8	81.7	88	97.4	21.5	20.3	1.06
		200	0.33	30.5	39	43.3	49.2	54.8	60.5	73.8	76.2	82.2	83.4	19.2	20.3	0.945
		400		42.4	47.6	48	53.1	56.7	69.4	70.2	71.9	82.5	85.8	10.2	20.3	0.503

Note: Values shaded red under the “Average Size per run” section indicate values over 130% over initial DLS reading. Values after the first red box were not included in the linear regression to calculate k_{exp}. Values shaded in red under the “k_{exp}” section indicate the k_{exp} values averaged to calculated k_{fast}.

Size versus time plots and 1/W (“alpha”) versus electrolyte concentration for each AgNP size and electrolyte combination

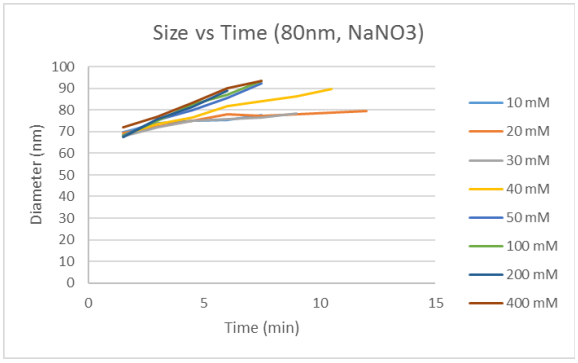

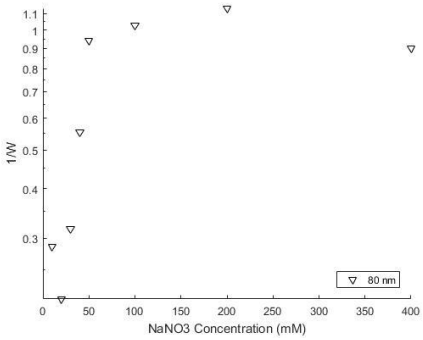

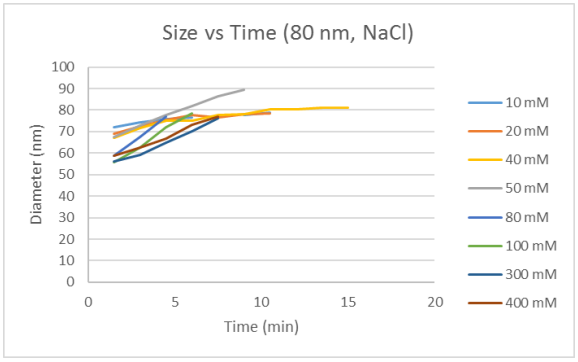

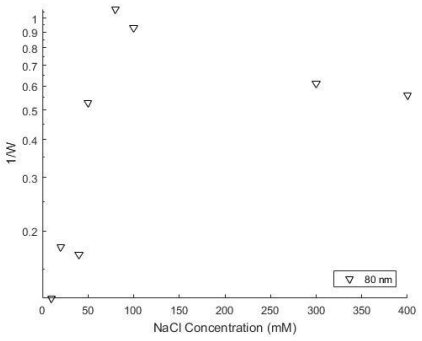

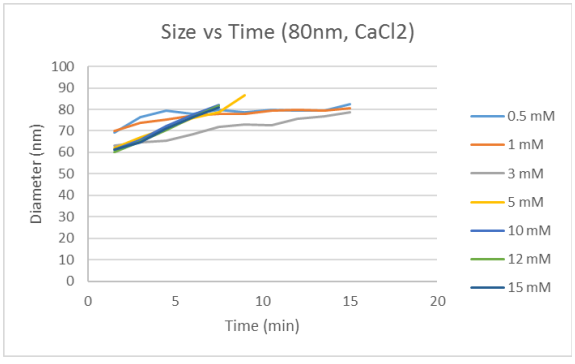

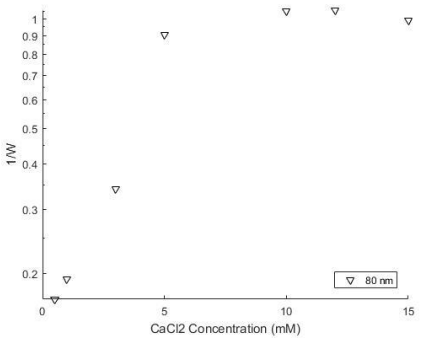

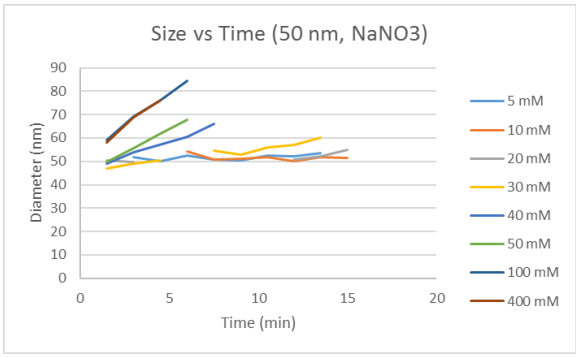
Size vs Time (50 nm, NaNO3)
Diameter (nm)
Time (min)
5 mM
10 mM
20 mM
30 mM
40 mM
50 mM
100 mM
400 mM

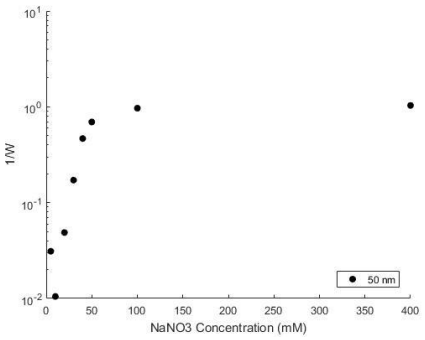
1/W
NaNO3 Concentration (mM)
50 nm

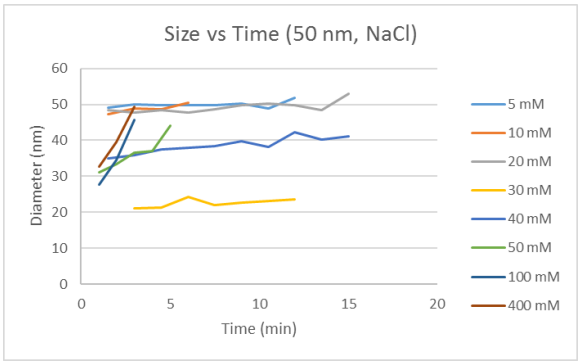
Size vs Time (50 nm, NaCl)
Diameter (nm)
Time (min)
5 mM
10 mM
20 mM
30 mM
40 mM
50 mM
100 mM
400 mM

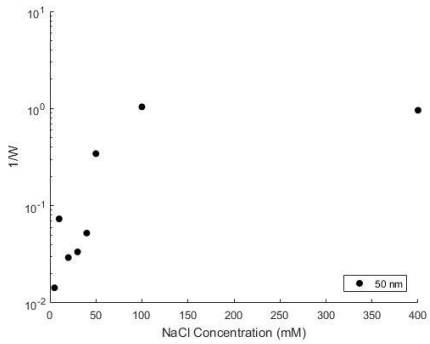
1/W
NaCl Concentration (mM)
50 nm

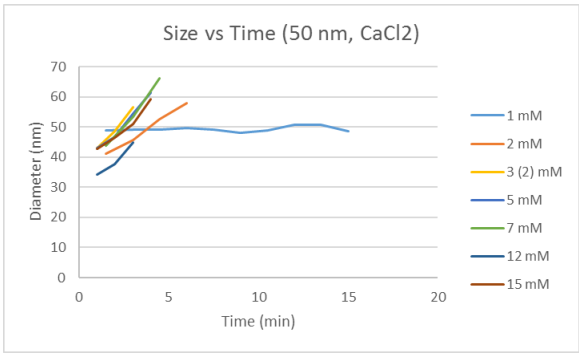
Size vs Time (50 nm, CaCl2)
Diameter (nm)
Time (min)
1 mM
2 mM
3 (2) mM
5 mM
7 mM
12 mM
15 mM

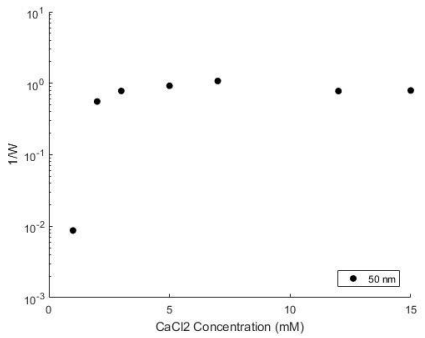
1/W
CaCl2 Concentration (mM)
50 nm

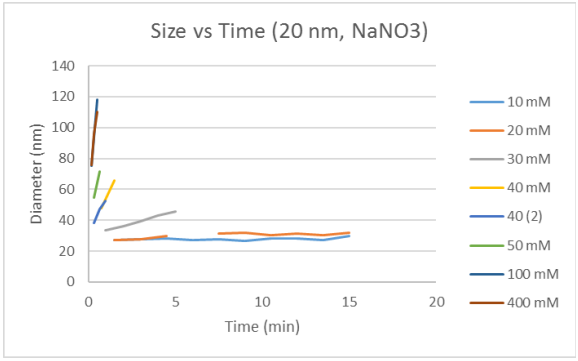
Size vs Time (20 nm, NaNO3)
Diameter (nm)
Time (min)
10 mM
20 mM
30 mM
40 mM
40 (2)
50 mM
100 mM
400 mM

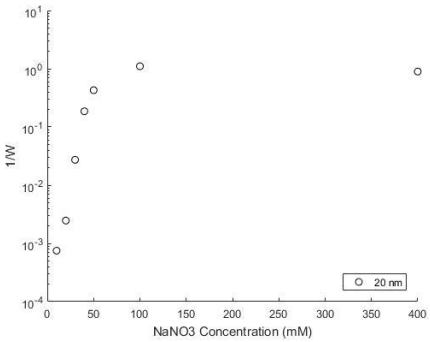
1/W
20 nm
NaNO3 Concentration (mM)

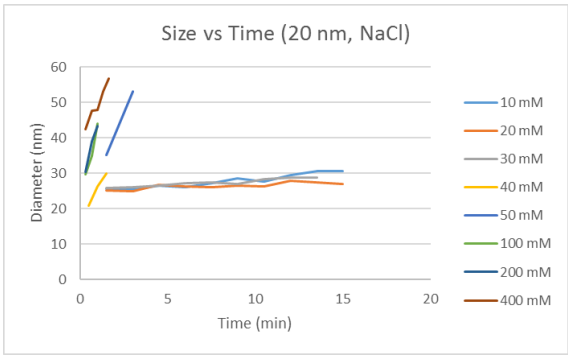
Size vs Time (20 nm, NaCl)
Diameter (nm)
Time (min)
10 mM
20 mM
30 mM
40 mM
50 mM
100 mM
200 mM
400 mM

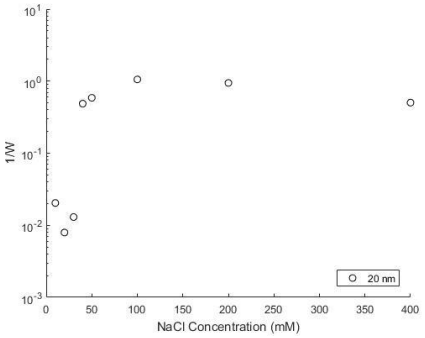
1/W
20 nm
NaCl Concentration (mM)

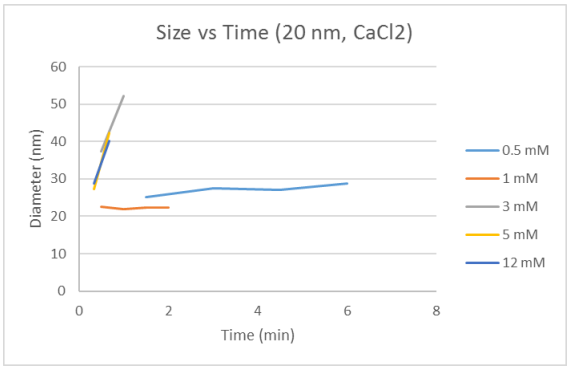
Size vs Time (20 nm, CaCl2)
Diameter (nm)
Time (min)
0.5 mM
1 mM
3 mM
5 mM
12 mM

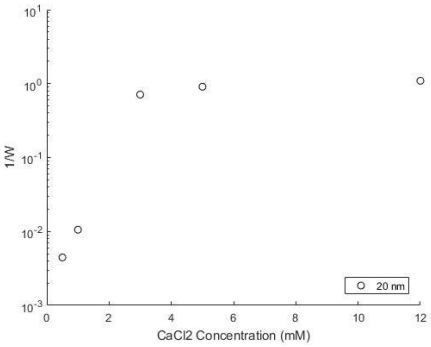
1/W
20 nm
CaCl2 Concentration (mM)